Heating of solid targets by subpicosecond laser pulses

W. Rozmus and V. T. Tikhonchuk*
Department of Physics, University of Alberta, Edmonton, Alberta, Canada T6G 2J1
(Received 13 July 1992)

Scaling laws for plasma temperature, thickness of the heated region, and other important plasma parameters are discussed for high-intensity subpicosecond laser plasma interactions with solid targets. Effects of inhibited heat fluxes are taken into account following recent formulations of the nonlocal thermal transport theories. It is shown that for constant laser intensities in excess of 10^{17} W/cm^2, i.e., in the anomalous skin-effect regime, plasma temperature increases much faster and to higher values for the inhibited thermal conductivity as compared to heating rates with the classical thermal transport. It it also shown, however, that the dynamical evolution of the heating process is primarily influenced by the time evolution of the laser intensity, which on the scale of ultrashort laser pulses makes the evolution of a plasma temperature almost identical for the classical and inhibited thermal transports.

PACS number(s): 52.50.Jm, 52.25.Fi

I. INTRODUCTION

The rapid progress in technology of short-pulse, high-intensity laser systems has led to many new applications in different areas, such as material sciences, development of x-ray sources, harmonic generation in ultraviolet light, and even in laser-induced nuclear reactions (cf. Ref. [1] for a recent review on these subjects). One of the main distinct characteristics of laser-plasma interaction processes on the subpicosecond scale is almost the entire lack of hydrodynamical evolution during the pulse duration. Therefore, for solid targets the laser energy can be directly deposited in the overdense plasma at solid densities, where the plasma temperature is defined by the balance between laser energy absorption in a skin layer, plasma heating, and thermal transport into cold and dense material.

In our previous study [2], we derived an analytical model for the ultrashort-pulse absorption in plasmas with a steplike density profile due to normal and anomalous skin effects. We have modeled a thermal transport by the classical Spitzer conductivity. The latter is only the first-order approximation, especially for the high laser intensities, when the characteristic dimensions of the heat wave are comparable with the electron collisional mean free path. It has also been shown in recent experiments [3–6] and by means of numerical Fokker-Planck calculations [7,8,3] that for laser intensities I_0 in the range of 10^{16}–10^{17} W/cm^2 and higher, the classical description of a thermal conductivity as a diffusion process is inadequate and one needs to include nonlocal kinetic effects.

In our present study we describe the model in which absorption of electromagnetic energy is balanced by the nonlocal thermal conductivity, as recently proposed by Epperlein and Short [9]. We discuss an alternative absorption coefficient and different scaling laws for important plasma parameters derived from the nonlocal thermal transport theory and compare them to our previous results [2] derived for the classical transport theory. Our formulation based on the Epperlein and Short model [9] includes both classical and inhibited thermal fluxes. The importance of the inhibited thermal conductivity becomes apparent during initial plasma evolution, when the temperature increases much more rapidly as compared to previous predictions [2] based on the Spitzer model. Our scaling laws compare well with the Fokker-Planck calculations. The effect of realistic intensity variations during the pulse duration on the temporal evolution of plasma temperature will also be discussed.

II. FORMULATION OF A HEATING MODEL WITH NONLOCAL HEAT FLOW

The starting point of our theory is the equation for electron temperature $T_e(z,t)$

$$\frac{\partial}{\partial t}(\tfrac{3}{2}n_e T_e)=\frac{\partial q}{\partial z} , \tag{1}$$

where the electron plasma density n_e is homogeneous in the half space ($z>0$). The frequency ω_0 of the short laser pulse interacting with solid density plasma is much smaller than the electron plasma frequency. Electron density n_e satisfies the relation $n_e \gg n_c$, where $n_c = m_e\omega_0^2/4\pi e^2$ is the critical density. Because the skin layer thickness is usually much smaller than the depth of a heated plasma region, we can consider the laser energy absorption in a plasma as a surface effect, which can be accounted for by the following boundary condition:

$$q(z=0,t)\equiv q_0(t)=AI_0 , \tag{2}$$

where I_0 is a laser intensity at $z=0$ and the absorption coefficient A is a function of temperature at the boundary $T(z=0,t)\equiv T_0(t)$ and therefore it implicitly depends on time.

The classical expression for the heat flux reads (SH denotes Spitzer-Harm)

$$q_{\rm SH}=\kappa_{\rm SH}T_e^{5/2}\frac{\partial T_e}{\partial z} , \tag{3}$$

where $\kappa_{\rm SH}=8(2/\pi)^{3/2}/Ze^4 m_e^{1/2}\Lambda$, Ze is the ion charge, and Λ is the Coulomb logarithm. This expression is valid for temperature profiles varying on the scale length longer than hundred electron mean free paths [10], and has been used before in description of subpicosecond laser target heating [2,6]. Our previous analysis [2], however, predicted temperature variations on a much shorter scale. Therefore we shall introduce in the present study an integral representation of the heat flux, which follows the formulations described before in Refs. [10,11,9],

$$q(z,t)=\int_{-\infty}^{+\infty} dz' G(z,z';t) q_{\mathrm{SH}}(z',t) , \qquad (4)$$

reproducing the Spitzer-Harm expression (3) in the classical limit. However, expression (4) can also properly account for the kinetic effects in the regime where the electron mean free path is comparable with the scale of the temperature gradient. The kernel G in (4) will be approximated by the formula recently proposed by Epperlein and Short [9], i.e.,

$$G(z,z';t)=\frac{1}{\pi a \lambda_e(z')}[-\sin\theta\,\mathrm{si}\theta-\cos\theta\,\mathrm{Ci}\theta] , \qquad (5)$$

where si and Ci are integral trigonometric functions [12], $\lambda_e=T_e^2/4\pi n_e e^4(Z+1)^{1/2}\Lambda$ is the electron mean free path, and for our case of constant homogeneous density $n_e=\mathrm{const}(z>0)$ argument $\theta=|z-z'|/a\lambda_e(z')$. The numerical constant $a=50$, found in Ref. [9], corresponds to values of the heat flux (4), which compare well with the results of Fokker-Planck calculations.

The important parameters describing laser light absorption and evolution of a solid target plasma are the electron temperature at the boundary $T_0(t)$ and the depth of a heat wave $z_f(t)$. We shall find the approximate behavior of these parameters from Eqs. (1)–(5). Later, we will also show that the temporal evolution of $T_0(t)$ and $z_f(t)$ depends very weakly on the actual spatial distribution of the temperature inside a plasma. Therefore we can assume the following form of a temperature profile:

$$T_e(z,t)=T_0(t)\eta(z/z_f(t)) , \qquad (6)$$

where η is a monotonically decreasing function, satisfying $\eta(0)=1$ and $\eta(\infty)=0$, and $z_f(t)$ is the penetration depth of a heat wave. After integrating Eq. (1) with respect to spatial variable z, one obtains the following equation for T_0 and z_f:

$$\frac{d}{dt}(T_0 z_f)=\frac{2}{3b_1 n_e}q_0(t) , \qquad (7)$$

where $b_1=\int_0^\infty \eta(\zeta)d\zeta$ is the constant of order unity that can be treated as a free parameter of our theory.

In order to close the system of Eqs. (2) and (7) one needs to express the heat flux $q_0(t)$ (4) in terms of T_0 and z_f. For small values of the temperature gradient ($z_f \gg a\lambda_e$), i.e., when T_e changes on the scale much longer than the scale of variations of the kernel G (5) in Eq. (4), one obtains a classical heat flux from Eq. (4). Calculating its value at the boundary $z=0$ with the help of Eq. (6), one obtains

$$q_0(t)=\tfrac{2}{3}b_3\frac{\kappa_{\mathrm{SH}}T_0^{7/2}(t)}{\pi z_f(t)} , \qquad (8)$$

where

$$b_3=\frac{3}{2}\left[\frac{d\eta}{d\zeta}\right]_{\zeta=0}\int_0^\infty d\theta[\sin\theta\,\mathrm{si}\theta+\cos\theta\,\mathrm{Ci}\theta]$$
$$\equiv -\frac{3\pi}{4}\left[\frac{d\eta}{d\zeta}\right]_{\zeta=0}$$

is the numerical constant. The plasma evolution for the case of classical thermal conductivity has been analyzed in our previous paper [2], where the regime of validity was restricted to relatively low laser intensities. Our present analysis includes also the opposite situation of higher intensities and hotter plasma when $z_f<a\lambda_e$ and a scale length of temperature variations is shorter or comparable with that of kernel G. For $z_f \ll a\lambda_e$ we can use an asymptotic expression for G (5) in the limit of $|\theta|\ll 1$

$$G(z=0,\zeta;t)=\frac{1}{\pi a\lambda_{e0}\eta^2(\zeta)}\ln\left[\frac{a\lambda_{e0}\eta^2(\zeta)}{z_f\zeta\mathcal{C}}\right] ,$$

where $\zeta=z'/z_f(t)$, λ_{e0} is the electron mean free path for temperature $T_e=T_0$ and $\mathcal{C}\approx 0.577$ is the Euler's constant. Substitution of the asymptotic form of G and the expression for the classical heat flux (3) into Eq. (4) and integration with respect to ζ result in the following form of the heat flux:

$$q_0(t)=\frac{2}{3}\frac{\kappa_{\mathrm{SH}}T_0^{7/2}(t)}{\pi a\lambda_{e0}(t)}\ln\left[b_2\frac{a\lambda_{e0}(t)}{z_f(t)}\right] , \qquad (9)$$

where the numerical coefficient $b_2\sim 1$ comes from integration of Eq. (4) over the heat wave thickness

$$b_2=\exp\left[-\frac{3}{2}\int_0^\infty d\zeta\,\eta^{1/2}\frac{d\eta}{d\zeta}\ln\left[\frac{\eta^2}{\mathcal{C}\zeta}\right]\right] .$$

Equation (9) is a convenient analytical approximation to the expression (4) valid in the limit of $z_f \ll a\lambda_{e0}$ and it will be used later to obtain scaling laws and analytical estimates. For practical applications, however, one also needs expression for the heat flux that is valid in the intermediate regime of $z_f \sim a\lambda_{e0}$ as well. We have calculated numerically the integral in Eq. (4) with the kernel G defined by (5) assuming various shapes of the temperature profile η (6). The results can be represented by the following expression:

$$q_0(t)=\frac{2}{3}\frac{\kappa_{\mathrm{SH}}T_0^{7/2}(t)}{\pi a\lambda_{e0}(t)}\left[\mathcal{F}\left[\frac{z_f(t)}{a\lambda_{e0}(t)}\right]\right]^{-1} , \qquad (10)$$

where, in principle, the function $\mathcal{F}$ depends on the particular choice of η. The function $\mathcal{F}$ has an asymptotic behavior corresponding to Eq. (9) for small values of the argument and for large arguments it gives the classical expression (8). As one can see from Fig. 1 the relatively simple logarithmic function

$$\mathcal{F}(x)=\left[\ln\left[\frac{b_2(1+x^2)+x(1+b_2b_3)}{x(1+b_2x)}\right]\right]^{-1} \qquad (11)$$

can very well approximate results of the numerical integration of Eq. (4) for arguments in a domain of practical interest $x \leq 2$. Figure 1 shows comparison between $\mathcal{F}(x)$ (11) and the results of numerical integration of Eq. (4) for $\eta(\zeta)=(1+\zeta)^{-2}$. We have also tried several other functions η that are equally well approximated by expression (11).

We will proceed with numerical integration of Eqs. (2), (7), and (10) to find the electron temperature and the absorption coefficient later in the paper. First, however, we shall analyze the approximate expression for the heat flux (9), which is valid for the strongly inhibited thermal transport when $z_f \ll a\lambda_e$. Comparing Eq. (9) with the expression for the classical heat flux Eq. (8) one finds an electron mean free path in the denominator of Eq. (9) replacing the actual temperature scale length in the classical thermal flux (8). This difference is responsible for the weak logarithmic dependence of q_0 (9) on z_f and also for the much weaker dependence on time of the temperature T_0 as compared to time variations of z_f. Assuming that the time derivative in the left-hand side of Eq. (7) acts only on the function $z_f(t)$ and taking constant in time laser intensity in Eq. (2) we derive an approximate expression for the depth of a heating front

$$z_f(t)=\frac{2A(T_0)}{3b_1 n_e T_0} I_0 t \ . \tag{12}$$

Substitution of this formula into Eqs. (2) and (9) leads to the equation for the plasma surface temperature

$$A(T_0)I_0=\frac{2}{3}\frac{\kappa_{\mathrm{SH}}}{\pi a}\frac{T_0^{7/2}}{\lambda_e(T_0)}\ln\left[\frac{3ab_1b_2n_eT_0\lambda_e(T_0)}{2A(T_0)I_0t}\right] . \tag{13}$$

The coefficients b_1 and b_2, containing information about the exact shape of the heat wave, appear in Eq. (13) only in the argument of the logarithmic function and therefore they have very small effect on our calculations of the electron temperature. For this reason we will neglect them altogether in the analytical expressions below [Eqs. (16)–(21)], taking $b_1=b_2=1$.

Nonlocal heat flow in the regime of the anomalous skin effect

We will derive an explicit expression for the absorption coefficient A, assuming that the plasma temperature is already high enough and the laser light absorption takes place in the regime of the anomalous skin effect, i.e., for

$$\omega_0/\omega_p < v_T/c \equiv (T_0/mc^2)^{1/2} \ . \tag{14}$$

In this case, the expression of the absorption coefficient at the normal laser incidence has been derived before (cf. Ref. [2])

$$A=1.4\left[\frac{\omega_0^2}{\omega_p^2}\frac{v_T}{c}\right]^{1/3} , \tag{15}$$

and it scales as $T_0^{1/2}$.

Using formula (15) for the absorption coefficient and solving Eq. (13) with the time-independent laser intensity I_0, we obtain the following scaling law:

$$T_0(t)\simeq T_* \ln^{-3/4}(t_*/t) \ , \tag{16}$$

where the characteristic plasma temperature

$$T_* \simeq 4.0 mc^2 Z^{3/8}\frac{\omega_0^2}{\omega_p^2}\left[\frac{I_0}{I_r}\right]^{3/4} \tag{17}$$

depends on the laser intensity ($I_r=mn_c c^3$ $=2.7\times10^{18}\lambda^{-2}$ W μm^2/cm^2 is the parameter describing relativistic laser flux) and the plasma density. The characteristic time scale related to an inhibited heat transport

$$t_* \simeq 9\pi a^2 n_e \lambda_e^2(T_*)/4\kappa_{\mathrm{SH}} T_*^{5/2} \tag{18}$$

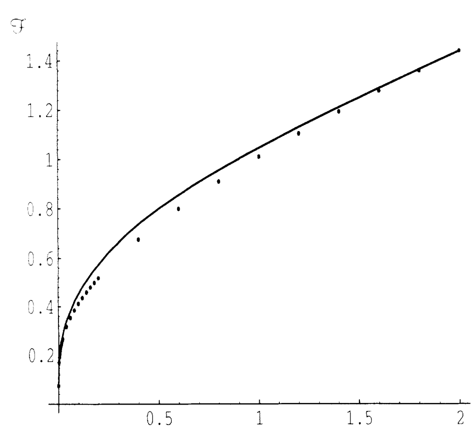

FIG. 1. Plot of the function $\mathcal{F}$ (11) ($b_2=0.66$, $b_3=3.03$) (solid line), compared with the results of numerical integration of Eq. (4) for the test temperature profile function $\eta(\zeta)=(1+\zeta)^{-2}$ (dots).

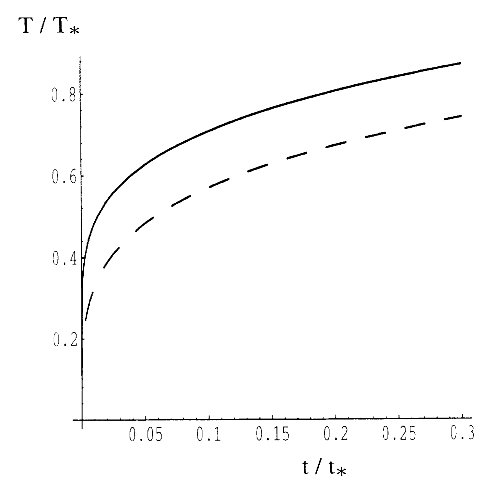

FIG. 2. Time evolution of electron temperature obtained from the solutions of Eqs. (2), (7), (10), and (15) for the constant laser intensity, in the anomalous skin-effect regime with the inhibited heat flux (solid curve). For comparison we also show temperature evolution with the classical heat flux (dashed line).

is approximately $a = 50$ times longer than the electron-ion collision time. Formulas (12) and (16)–(18) describe also the propagation of a heat wave

$$z_f(t) \simeq z_* \frac{t}{t_*} \ln^{5/8} \left[\frac{t_*}{t} \right], \tag{19}$$

where $z_* = a\lambda_e(T_*)$. The thickness of a heated region increases approximately linearly with time and corresponds to nearly collisionless propagation of heated electrons from the boundary into the plasma.

Expressions (16)–(19) constitute important results of this study. They predict very fast temperature growth during the initial stage of interaction dominated by the inhibited thermal transport. The region of their applicability, however, is restricted to very short times of the order of $t \ll t_*$. For longer times we have used the interpolation formula (10) and we have solved Eqs. (2) and (7) numerically. The results are illustrated in Fig. 2, where the temporal dependence of the plasma temperature has been shown for the time-independent laser intensity. As one can see after initial rapid increase, the temperature growth levels off at approximately $t \sim 0.1t_*$. Also comparison with the temperature evolution for the classical thermal flux (dashed curve in Fig. 2) shows, as expected, faster temperature growth for the inhibited heat fluxes. Plots shown in Fig. 2 have been obtained with the simplified assumption about the spatial temperature profile η (6), i.e., by taking $b_1 = b_2 = b_3 = 1$ in Eqs. (10) and (11). We have repeated this analysis with different functions η, finding each time similar results for the temperature and its temporal dependence. As we already noticed before, the actual form of the temperature profile has small effect on the evolution plasma parameters.

The fast time response of the plasma temperature shown in Fig. 2 for the constant laser intensity suggests that in a more realistic situation of the time varying laser intensity, a time evolution of the temperature will closely follow variations of a laser pulse. We have solved again Eqs. (2), (7), and (10) assuming time-dependent laser pulse of the following form:

$$I_0(t) = I_0[\sin(\pi t/\tau_0)]^2 . \tag{20}$$

The results are shown in Figs. 3 and 4 for different durations of a laser pulse $\tau_0 = 0.3t_*$ and $\tau_0 = 0.1t_*$, respectively. As in Fig. 2 we have also shown, for comparison, results obtained for the classical heat flux (dashed curves). As expected, temperature follows very closely time evolution of the laser pulse and reaches zero values of the vanishing laser intensity. Also finite extent and time variation of the laser pulse result in evolutions of electron temperature, which are almost identical for the classical and inhibited thermal conductivities.

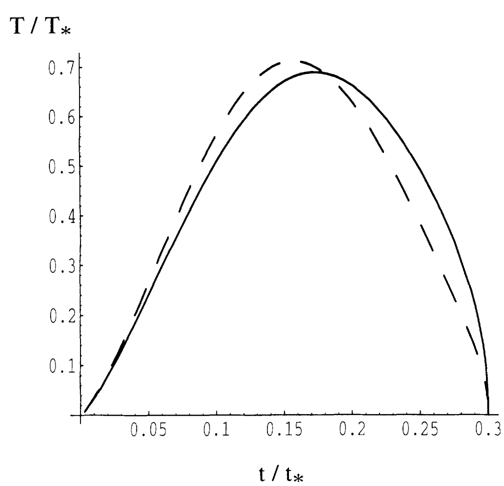

FIG. 3. Time dependence of the plasma temperature obtained from the solutions of Eqs. (2), (7), (10), and (15) for the laser pulse (20) with the time duration $\tau_0 = 0.3t_*$ (solid line). The dashed curve shows results obtained for the same parameters but with the classical heat flux.

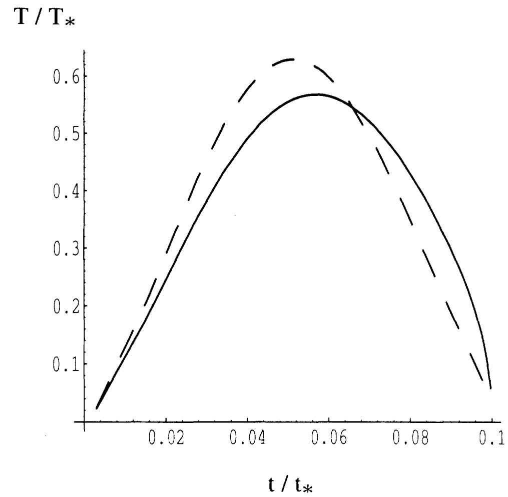

FIG. 4. Time dependence of the plasma temperature obtained from the solutions of Eqs. (2), (7), (10), and (15) for the laser pulse (20) with the time duration $\tau_0 = 0.1t_*$ (solid line). The dashed curve shows results obtained for the same parameters but with the classical heat flux.

III. DISCUSSION AND CONCLUSIONS

To summarize our results for the anomalous skin effect we will express them in dimensional units, i.e., temperature in keV, length in μm, and time in ps. Taking the Coulomb logarithm $\Lambda = 5$, assuming the solid-state density for ions $n_i = 6 \times 10^{22}$ cm^{-3} and $n_e = Zn_i$, we have

$$\begin{aligned} T_* &= 16 Z^{-5/8} \lambda^{-1/2} I^{3/4} \text{ keV} , \\ t_* &= 90 Z^{-2} \lambda^{-3/4} I^{9/8} \text{ ps} , \\ z_* &= 5 \cdot 10^3 Z^{-11/4} \lambda^{-1} I^{3/2} \ \mu\text{m} , \end{aligned} \tag{21}$$

where λ is the laser wavelength expressed in microns and $I = I_0 \times 10^{-18}$ W/cm^2 is the normalized laser intensity. The absorption coefficient (15) exhibits very weak time dependence $A = A_* \ln^{-1/8}(t_*/t)$ for $t \ll 0.1t_*$ and the characteristic value

$$A_* = 0.7 Z^{-1/2} \lambda^{-3/4} I^{1/8} \tag{22}$$

depends mainly on Z and laser wavelength but only very weakly on the laser intensity. Expressions (21) and (22) approximate reasonably well plasma parameters for $t < t_*$, and for longer times asymptotic behavior of plasma parameters has been derived for the classical heat flux and is given in Ref. [2] [cf. Eq. (66) in [2]].

Expressions (21) predict reasonable values for plasma parameters. Taking as a typical example laser intensity $I_0 = 10^{18}$ W/cm^2, wavelength $\lambda = 0.5$ μm, and $Z = 10$ we obtain from Eqs. (21) and (22) $T_* = 5.4$ keV, $z_* = 18$ μm, and $A_* = 9\%$. The characteristic time $t_* = 2.3$ ps is longer than the duration of the present ultrashort-laser pulses [1,3,4,5], and as we will see below, the real limitation on the extent of the anomalous skin-effect regime is given by the time of hydrodynamical expansion. These numerical values are also in good agreement with the results of Fokker-Planck simulations of the dense plasma heating presented in Ref. [7].

The characteristic time t_* is of order of the collision time, which is much longer than the laser period. Therefore studying absorption processes on the scale of $t < t_*$ we could neglect collisions and account only for the anomalous skin effect. At the same time the inequality (14) is only marginally satisfied and $\omega_0/\omega_p \sim v_T/c$. This means that mainly thermal electrons participate in the laser light absorption and formula (15) may underestimate the value of the absorption coefficient. On the other hand more accurate description of the absorption process requires detailed information about the distribution function of heated electrons, which is out of the scope of our simple analytical theory.

The region of applicability of our results, in particular of the expressions obtained for the anomalous skin effect, is defined by the characteristic time scale t_*, which is longer than the laser pulse duration τ_0 and shorter than the time $\tau_{\rm ion}$ of the hydrodynamical expansion. The first condition defines the minimum laser intensity corresponding to the collisionless absorption process

$$I_0 \geq Z^2 \tau_0 \lambda^{3/4} \times 10^{16} \text{ W/cm}^2 \; .$$

As before, the pulse duration τ_0 is expressed in picoseconds and wavelength λ in micrometers. The second restriction, related to ion motion, defines the upper limit on the laser pulse duration. According to our previous study [2], the hydrodynamic expansion becomes important when the plasma inhomogeneity scale length $L = (zT_e/\mathcal{A} m_H)^{1/2} t$, where $\mathcal{A}$ is the atomic mass number and m_H is the mass of a hydrogen atom, equals to the plasma skin length. Using Eqs. (21) one can find that the hydrodynamic motion can be neglected if

$$\tau_0 < 0.17 \lambda^{3/11} \mathcal{A}^{9/22} Z^{-19/22} \text{ ps} \; .$$

This is the most severe restriction of our theory, derived for the steplike density profile. For longer pulses the absorbing region shifts from overdense plasma toward critical density with the corresponding change in the absorption mechanism. Instead of collisionless effects discussed above inverse Bremsstrahlung absorption becomes more important. Also the amplitude of the laser electric field in the absorption region increases and may lead to various nonlinear effects. These new effects related to the finite density gradient may still be included in the theoretical approach outlined in this paper for the steplike density profile by changing an effective absorption coefficient.

ACKNOWLEDGMENTS

We thank Mary Yiu for a careful reading of this paper. This work was partly supported by the Natural Sciences and Engineering Research Council of Canada.

*On leave from P. N. Lebedev Physics Institute, Russian Academy of Sciences, Moscow, Russia.

[1] B. Luther-Davies, E. G. Gamaly, Y. Wang, A. Rode, and V. T. Tikhonchuk, Laser Phys. **1**, 325 (1991).
[2] W. Rozmus and V. T. Tikhonchuk, Phys. Rev. A **42**, 7401 (1990).
[3] A. Zigler, P. G. Burkhalter, D. J. Nagel, M. D. Rosen, K. Boyer, T. S. Luk, A. McPeterson, and C. K. Rhodes, Opt. Lett. **16**, 1261 (1991).
[4] J. D. Kmetec, C. L. Gordon, III, J. J. Macklin, B. F. Lemoff, G. S. Brown, and S. E. Harris, Phys. Rev. Lett. **68**, 1527 (1992).
[5] G. A. Kyrala, R. D. Fulton, E. K. Wahlin, L. A. Jones, G. T. Schappert, J. A. Cobble, and A. J. Taylor, Appl. Phys. Lett. **60**, 2195 (1992).
[6] R. Fedosejevs, R. Ottmann, R. Sigel, G. Kuhnle, S. Szatmari, and F. P. Schafer, Appl. Phys. B **50**, 79 (1990).
[7] A. A. Andreev, E. G. Gamaly, V. N. Novikov, A. N. Semakhin, and V. T. Tikhonchuk, Zh. Eksp. Teor. Fiz. **101**, 1808 (1992) [Sov. Phys.—JETP **74**, 963 (1992)].
[8] J. M. Wallace, D. W. Forslund, J. M. Kindel, G. L. Olson, and J. C. Comly, Phys. Fluids B **3**, 2337 (1991).
[9] E. M. Epperlein and R. W. Short, Phys. Fluids B **3**, 3092 (1991).
[10] J. F. Luciani, P. Mora, and J. Virmont, Phys. Rev. Lett. **51**, 1664 (1983).
[11] J. R. Albritton, E. A. Williams, and K. P. Shwartz, Phys. Rev. Lett. **57**, 1887 (1986).
[12] I. S. Gradshtein and I. M. Ryzhik, *Table of Integrals, Series, and Products,* translated and edited by A. Jeffrey (Academic, New York, 1980), p. 928.